*Malaysian Journal of Chemistry, 2015, Vol. 17(2), 16–28*

# Removal of Malachite Green from Aqueous Solution by Waste Tyre Derived Activated Carbon

**C. G. Joseph[1]*, J. Janaun[2] and M. Massuanna[1]**

[1] Water Research Unit, Faculty of Science and Natural Resources, Universiti Malaysia Sabah, Jalan UMS, 88400 Kota Kinabalu, Sabah, Malaysia.
[2] Chemical Engineering Program, Faculty of Engineering, Universiti Malaysia Sabah, Jalan UMS, 88400 Kota Kinabalu, Sabah, Malaysia

*Corresponding author (e-mail: collin@ums.edu.my)

Waste rubber tyres were used to prepare activated carbon via destructive distillation method employing a two stage process i.e. carbonization and chemical activation in a tubular furnace. Carbonization was done at 500°C for 1 h followed by impregnation of char with NaOH. Activation was done in a horizontal tube furnace via $CO_2$ activation. Two variables and three parameters i.e. impregnation ratio between NaOH and char (1:1 and 3:1), activation temperature (700°C and 900°C), and activation time (60 min and 180 min) were studied and its effects on percentage yield, and malachite green (MG) dye removal were compared and presented in this paper. IR spectra of all samples a number of bands at 1710, 1620, and 1054 $cm^{-1}$ –1026 $cm^{-1}$ which proved the presence of carboxylic, carbonyl, and some acids, alcohols, ether and ester groups on the surface of carbon prepared. Activated carbon, AC6, which was prepared at ratio 3:1 and heated at 900°C for 60 min preparation was selected due to high surface area (313.17 $m^2/g$) and removed about 97.43% of MG dye after 60 min. AC6 was best fitted to the Freundlich isotherm indicating multilayer adsorption while the adsorption kinetic followed pseudo-second order kinetics. The maximum monolayer adsorption was 128.21 mg/g.

**Key words:** Activated carbon; adsorption; malachite green; waste tyre; impregnation ratio

*Received: April 2015; Accepted: September 2015*

Malachite green (MG) is a basic dye which is categorized as triphenylmethane dye and appears as green crystalline powder and is easily dissolved in water. MG is used as antifungal agent in aquatic systems such as fish hatcheries, and also dyeing of leather, silk and wool; however, MG dye has been reported to be highly toxic and carcinogenic [1,2]. It has been banned in some countries such as USA and Japan since 1967. However, in Malaysia, there has been no specific law regulated by the government regarding the concerns on this issue [3]. Therefore, adsorption process is one of the selected methods, which is well-known as an economical and effective method for the removal of MG dye.

Each year, it is estimated that about 1.5 billion tyres are produced worldwide which ends up as waste [4]. Major problems that have arisen have been discussed in previous study [5], such as tyres tend to provide breeding areas for mosquitoes which causes health complications, a large stockpile could consequently cause uncontrolled fire hazard, and disposal of waste tyres is becoming more expensive which in turn, causes illegal dumping. Waste tyres have high content of volatile matter, which makes them as interesting solidfuel for energy production and in pyrolysis products which allows the transformation of tyres into three useful classes of products: a solid, a liquid and a gas [6]. Pyrolysis of waste tyre produces

about 30% – 40% of solid product [7] which can be further treated into activated carbon either by chemical or physical activation [8]. Waste tyres as activated carbon has been used as adsorbent in removal of phenolic compound [9], chromium [10], reactive dye [11] and many more.

Previous researchers have prepared activated carbon from waste tyre by means of chemical activation using KOH [12], $ZnCl_2$ and $H_3PO_4$ [13], and treatment with $HNO_3$ to increase the oxygen group [14]. NaOH has been used as an activating agent for carbon derived from cherry stone [15], rice husk [16], Jatropha curcas seed [17] and peanut shells [18]. Cazetta *et al*. [19] stated that among the basic reagents, NaOH activation in comparison with KOH activation has advantages such as: (i) lower dosage (weight measurement), (ii) cheaper; (iii) more environmentally friendly; and (iv) less corrosive. In physical activation, $CO_2$ activation is an effective method in preparing porous activated carbon. Activation of peanut shells by chemical activating agent via $CO_2$ activation produced a porous carbon with high surface area (1060 $m^2/g$) and a good adsorbent for methylene blue and phenazone removal [18]. Hamad *et al*. [3] prepared oil palm shell activated carbon (OPSAC) impregnated with NaOH then activated via $CO_2$ activation. OPSAC produced has 2247 $m^2/g$ surface area and was tested for its application as an adsorbent for removal of 4-chloroguaiacol (4CG). Activation of tyres using NaOH as activating agent via $CO_2$ activation has not been reported.

This research aims to produce activated carbon from waste tyre impregnated with NaOH via $CO_2$ activation, and evaluate its potential as an adsorbent for the removal of MG dye. The effects of various parameters during carbon preparation, such as activation temperature, impregnation ratio, and time, on carbon yield and MG dye removal were investigated. Two different models of isotherm and kinetic studies were performed to evaluate the capability of tyre activated carbon to adsorb the MG dye.

## EXPERIMENTAL STUDY

### Material

The outside rubber tyres (treads area) were cut into small pieces between 2–3 mm. The rubber tyre was cleaned and dried in an oven for 24 h at 105°C. MG oxalate was supplied by Sigma Sdn Bhd (Malaysia) and used as provided.

### Carbon Production

Two production stages of activated carbon were used in this study i.e. carbonization and activation. In the carbonization step, 100 g of rubber tyre was placed in stainless steel crucible and loaded into high temperature muffle furnace, HF 3.8-1700 – CMTS Model. The rubber tyre was heated at 500°C for 1 h to remove volatile matter under self-generated atmosphere method. After that, the char produced was impregnated with activating agent, NaOH at the different ratio (NaOH:char) for 48 h at 65°C and 140 rpm.

Activation step was done by loading the impregnated char into Single Split Horizontal Tubular Furnace. The samples were heated under $N_2$ flow at a flow rate of 150 ml/min for 1 h then followed by $CO_2$ with flow rate of 150 ml/min for different activation temperatures (700°C and 900°C) and time (60 min and 180 min). After cooling, the resulting product was washed with 1M of HCl followed by hot distilled water until the pH reach ~5.5. The sample was dried in an oven at 105°C for 24 h. The parameters studied are listed in Table 1.

## CHARACTERISTIC

*Percentage yield*. The percentage yield of the activated carbon prepared was calculated according to Equation 1:

$$\text{Yield (\%)} = \frac{x}{y} \times 100 \quad (1)$$

where $x$ is the amount of activated carbon produced (g), and $y$ is the amount of raw material (g).

*Ash content*. In order to analyse the ash content of activated carbon, 1.0 g of activated carbon was placed in a crucible and heated up to 400°C in muffle furnace. After 3h, the sample was cooled down to room temperature and weighed. The ash content percentage was measured according to Equation 2 [20]:

$$\text{Ash content (\%)} = \frac{\text{Weight after heating}}{\text{Weight before heating}} \times 100 \quad (2)$$

*Moisture content*. Approximately 1.0 g of activated carbon was heated in an oven at 120°C. After 2 h, the sample was placed in desiccator and weighed according to Equation 3 [20]:

$$\text{Moisture content (\%)} = \frac{\text{Weight after drying}}{\text{Weight before drying}} \times 100 \quad (3)$$

*Surface area and pore size distribution*. $N_2$ adsorption-desorption isotherm was measured to determine the properties of pores and the surface area of the activated carbon. Brunauer-Emmett-Teller (BET) and surface area analysis were conducted at SIRIM's Advanced Materials Research Centre (AMREC) in Kulim, Kedah.

*Functional group*. The IR spectrums of all samples (AC1-AC8) were recorded using Perkin-Elmer FTIR Spectrometer in the range of 4000 $cm^{-1}$ to 650 $cm^{-1}$ to study the functional groups.

### Adsorption Experiment

Batch experiments were conducted in order to study the behaviour of MG in an aqueous solution. In this experiment, 0.02 g of activated carbon prepared (AC1-AC8) was added into a 250 ml beaker containing 200 ml of 10 mg/l of MG dye solution without adjusting pH [21]. The initial pH of MG dye was 5.59±0.08. The beaker was stirred at room temperature. The contact time was selected at 60 min according to the preliminary experiment for all equilibrium tests. To study the effect of initial concentration, 0.02 g of activated carbon prepared were added at five different concentrations (2, 4, 6, 8, and 10 mg/l). Small amount of solution was filtered and the supernatant was analysed by measuring the absorbance value at wavelength of 617 nm using Eppendorf BioSpectrometer kinetic. The amount of MG adsorbed, $q_e$ (mg/g) was calculated using Equation 4:

$$q_e = \frac{(C_i - C_e)V}{m} \quad (4)$$

where $C_i$ and $C_e$ are the initial and equilibrium concentrations of the MG solution (mg/l) respectively, $V$ is the volume of solution (L), and $m$ is the mass of the adsorbent (g).

## RESULTS AND DISCUSSION

### Characteristics of Activated Carbon

*Percentage yield.*

Effect of impregnation ratio.

Table 1 shows the effect of impregnation ratio of NaOH to char at 1:1 and 3:1. As the impregnation ratio increased from 1 to 3, the yield of carbon produced decreased. At constant temperature and time, the decrease in yield percentage was observed to have similar trend for different impregnation ratio as compared between samples AC1 (76.10%) to AC2 (51.63%), AC3 (65.99%) to AC4 (47.31%), AC5 (44.06) to AC6 (30.22%), as well as AC7 (12.95%) to AC8 (7.17%). Similar trend was reported in the previous study [8] in the activation of tyre using $ZnCl_2$. This is because during the activation process, dehydrating reagent (NaOH) reacted and provided elimination reaction breaking the bonds of C-O-C and C-C of the char [19].

Effect of activation temperature.

Activation temperature is one of the factors influencing the percentage yield. From Table 1, the percentage yield of carbon decreased as temperature increased from 700°C to 900°C. In comparison, AC1 (76.09%), AC2 (51.63%), AC3 (65.98), and AC4 (47.31%) prepared at 700°C have higher percentage yield than AC5 (44.06%), AC6 (30.22%), AC7 (12.95%), and AC8 (7.17%) which

**Table 1.** The percentage yield, moisture and ash content of samples prepared.

| Samples | Temperature (°C) | Ratio of NaOH to char (g/g) | Time (min) | Percentage yield (%) | Moisture content (%) | Ash content (%) |
|---|---|---|---|---|---|---|
| AC1 | 700 | 1 | 60 | 76.09 | 2.09 | 13.09 |
| AC2 | 700 | 3 | 60 | 51.63 | 2.72 | 12.52 |
| AC3 | 700 | 1 | 180 | 65.98 | 1.09 | 10.97 |
| AC4 | 700 | 3 | 180 | 47.31 | 3.29 | 10.66 |
| AC5 | 900 | 1 | 60 | 44.06 | 2.76 | 9.73 |
| AC6 | 900 | 3 | 60 | 30.22 | 1.73 | 10.13 |
| AC7 | 900 | 1 | 180 | 12.95 | 3.33 | 9.89 |
| AC8 | 900 | 3 | 180 | 7.17 | 1.43 | 9.01 |

were prepared at 900°C for same impregnation ratio and activation time. Teng *et al*. [13] produced activated carbon from tyres using KOH found the decreasing of carbon yield from 26% to 11% as temperature increased from 600°C to 900°C. This is due to the increased carbon gasification by $CO_2$ or oxygen in the alkali. The evolved $CO_2$ can react with carbon atoms to open up closed pores and enlarge the existing micropores, resulting in increased porosity.

Effect of activation time.

Effects of activation time on activated carbon prepared was investigated in which $CO_2$ gas introduced to sample after 1 h heating by N2 gas during activation step. Based on Table 1, as the activation time increased from 60 min to 180 min, the percentage yield decreased. AC1-AC2 (76.09% – 51.63%) prepared at 60 min produced higher carbon yield compared to AC3-AC4 prepared at 180 min (65.98% – 47.31%). Similar trend was observed for AC5-AC6 (47.31 – 44.06%) when compared to AC7-AC8 (30.22% – 1.95%). This might be due to the sintering effect, which considerably destroyed the pore between the adjacent pore [21] and increased the burn off effect giving low percentage yield.

*Moisture content*. The amount of moisture content is listed in Table 1. Overall moisture content observed was less than 10%. AC3 had the lowest moisture content which was 1.09% and the highest was AC7 with 3.33%. Based on the results obtained, parameters study did not influence the moisture content of carbon. Previous study suggested that there is no correlation between moisture content and adsorption power of carbon [22].

*Ash content*. Ash is defined as the amount of impurity of a substance which is left as residue after a complete combustion of the carbon. Table 1 lists the ash contents of tyre activated carbon produced. It shows that the ash content of activated carbon prepared varied from 8.34% to 15.24%. Chan *et al*. [23] produced activated carbon with about 6% to 28% of ash content. They stated that the accumulation of the inorganic matter left in the char results in the increase of ash content during the activation process.

*$N_2$ adsorption-desorption*. Figure 1 shows the $N_2$ adsorption-desorption isotherm of all samples prepared, and the adsorption of $N_2$ gas at relatively low pressure. All samples were characterized as type IV isotherms which showed the hysteresis loop characteristics of mesopore. Similar finding was observed in previous studies [24,25] on the pyrolysis of tyres.

The surface physical parameters obtained from $N_2$ adsorption isotherms were summarized in Table 2. From the data, AC6 had higher surface area (313.75 $m^2/g$) compared to other samples. AC8 had the lowest surface area (144.78 $m^2/g$). This was influenced by the method of preparation as mentioned above. The pores of all samples consolidated in the range of 20Å to 50Å, which

**Table 2.** The porous and surface properties of samples.

| Samples | $S_{Bet}$ ($m^2/g$) | Total pore volume (cc/g) | Micropore volume (cc/g) | Mesopore volume (cc/g) | Pore diameter (Å) |
|---|---|---|---|---|---|
| AC1 | 156.56 | 1.03 | 0.06 | 0.96 | 261.90 |
| AC2 | 298.96 | 1.05 | 0.13 | 0.92 | 140.20 |
| AC3 | 132.99 | 0.91 | 0.05 | 0.86 | 274.70 |
| AC4 | 180.19 | 1.06 | 0.01 | 1.05 | 234.70 |
| AC5 | 207.84 | 1.02 | 0.01 | 1.01 | 195.50 |
| AC6 | 313.75 | 1.25 | 0.13 | 1.12 | 159.00 |
| AC7 | 173.58 | 0.84 | 0.07 | 0.77 | 193.80 |
| AC8 | 144.78 | 0.50 | 0.06 | 0.44 | 152.00 |

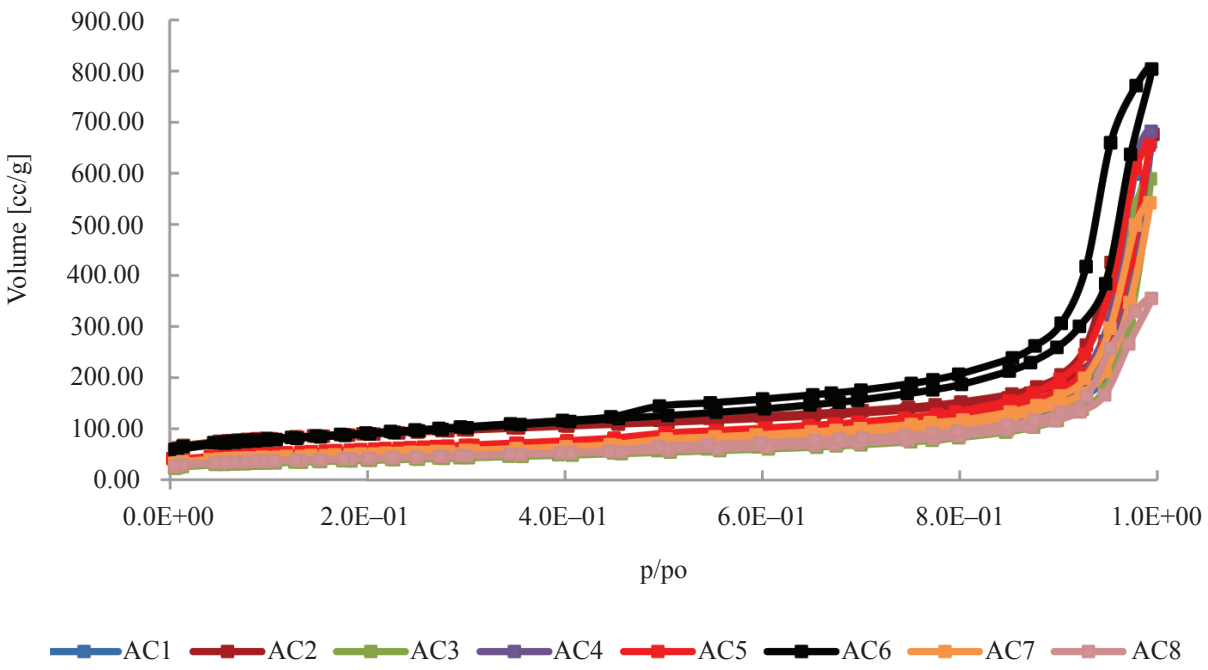


**Figure 1.** $N_2$ Adsorption-desorption.

corresponded to the mesopore range. This was also supported by the fact that the amount of mesopore volume in sample (as in Table 2) was more than half the amount of total pore volume.

*Functional group*. Figure 2 shows the IR spectra for all activated carbon derived from waste tyres display a frequently weak band. This might be due to removal of organic functional groups during the manufacturing of the tyres. All samples presented similar patterns and functional groups due to the same precursor and activating agent used. The weak broadband located at 3924 $cm^{-1}$–3600 $cm^{-1}$ was attributed to the presence of O-H stretching vibration of hydroxyl group [26]. As temperature increased from 700(AC1-AC4) to 900°C (AC5-AC8) the broadband appeared at 3000 $cm^{-1}$–2850 $cm^{-1}$ indicated the stretching of C-H in alkanes. The weak bands at 2420 $cm^{-1}$–2333 $cm^{-1}$ were attributed to the stretching CΞC vibrations in alkynes groups [26]. The strong bands observed at 1710 $cm^{-1}$–1621 $cm^{-1}$ were attributed to the stretching of C=O vibrations carboxyl and carbonyl in acidic oxygen group [27]. The bands

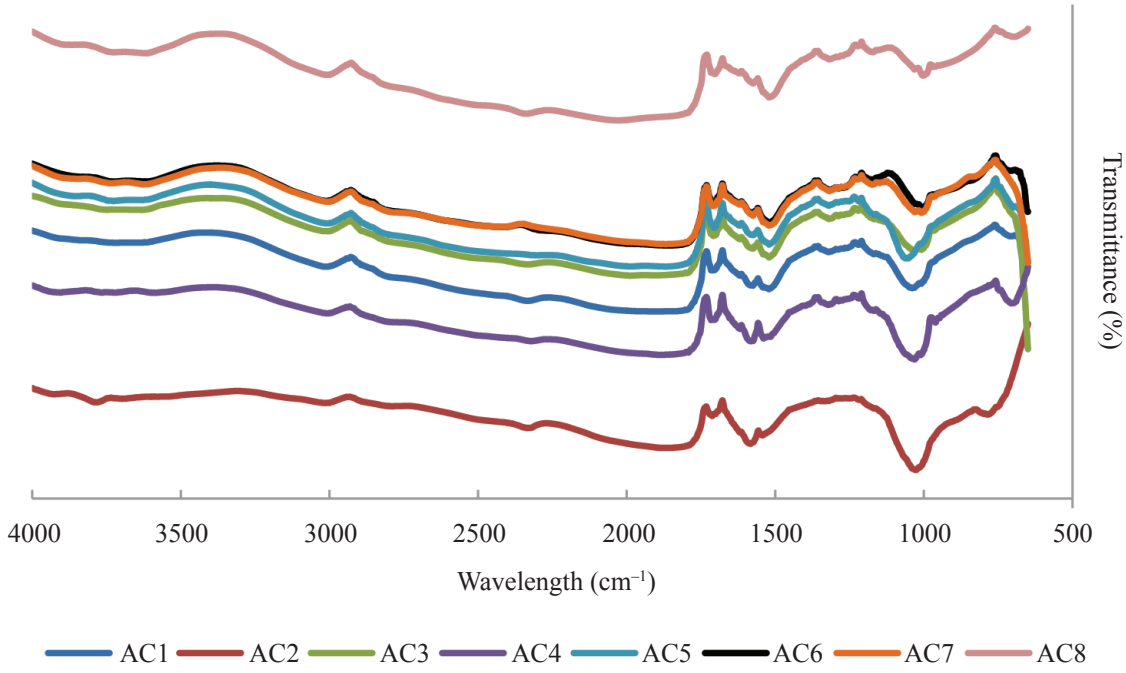


**Figure 2.** FTIR spectra of activated carbon prepared.

at 1320 $cm^{-1}$–1316 $cm^{-1}$ were attributed to C-H bending in alkanes or alkyl groups [3]. The bands at 1054 $cm^{-1}$–1026 $cm^{-1}$ were attributed to the C-O stretching in acids, alcohols, phenols, ether and ester [28]. The band at 961 $cm^{-1}$ and 786 $cm^{-1}$–697 $cm^{-1}$ were corresponding to the presence of aromatic C-H in a plane-bending and out-of-plane bending, respectively [29]. The series of samples prepared at 900°C (AC5-AC8) showed decreased intensity compared to samples prepared at 700°C (AC1-AC4) proving the parameter study affected the chemical properties of carbon.

## Adsorption of MG onto Activated Carbon

Figure 3 shows the adsorption of 10 mg/l of MG dye onto various activated carbons prepared. At the early stages, the rapid uptake of MG dye adsorbed were observed at the first 30 min, and slowly reached equilibrium at 60 min. This trend was observed for samples AC1, AC3, AC4, AC5, AC7, and AC8. While, AC2 and AC6 adsorbed MG dye rapidly at early 40 minutes, then reach equilibrium at 60 minutes. The fast uptake on the first stage was due to the creation of more activated sites on the surface of activated carbons prepared. AC6 prepared at 900°C, impregnation ratio 3:1, and activation time 60 min was the best sample prepared which presented the highest adsorption capacity of MG dye at 60 min, 100.09 mg/g. This was also supported by the value of surface area as presented in Table 2. The order of adsorption capacity followed from AC8 <AC3 <AC1 <AC7 <AC4 <AC5 <AC2 and AC6.

## Effect of Initial Concentration

The effect of initial concentration of MG dye was investigated. AC6 was selected due to high surface area as well as high adsorptive capability. The various concentrations studied in this experiment ranges from 2 mg/l to 10 mg/l of MG dye. As shown in Figures 4 and 5, the contact time required for lower initial concentration of MG dye (2, 4 and 6 mg/l) to reach equilibrium was 30 min, while for initial concentration 8 mg/l and 10 mg/l required 45 min and 50 min to reach equilibrium, respectively. An increase in the initial concentration (2 mg/l–10 mg/l) increases the amount of MG dye (18.66 mg/g–100.09 mg/g). Similar finding was observed in a previous study [30] which adsorbed MG dye using Copper Nanowires (Cu-NWs) activated carbon. They explained that the higher initial concentration of MG dye provides an important

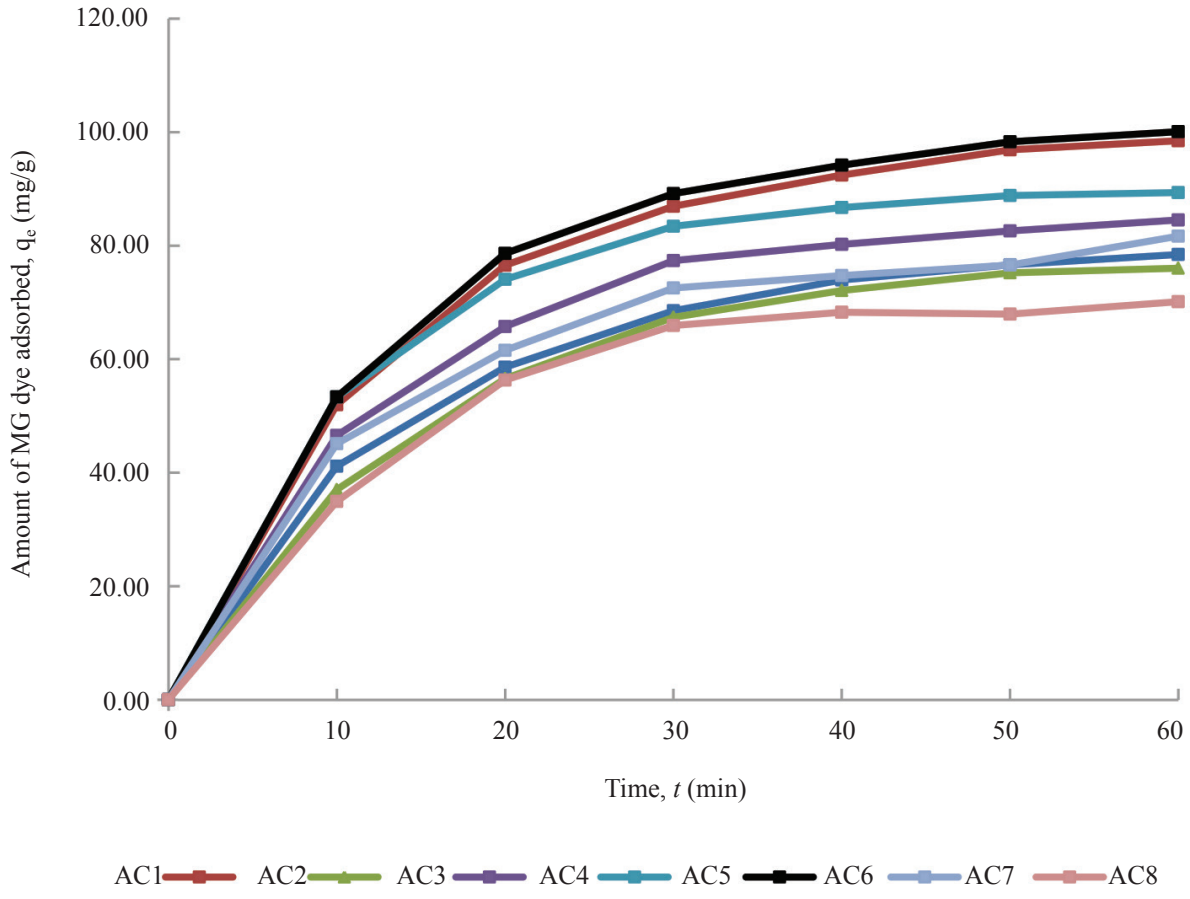


**Figure 3.** Adsorption Equilibrium of activated carbon prepared.

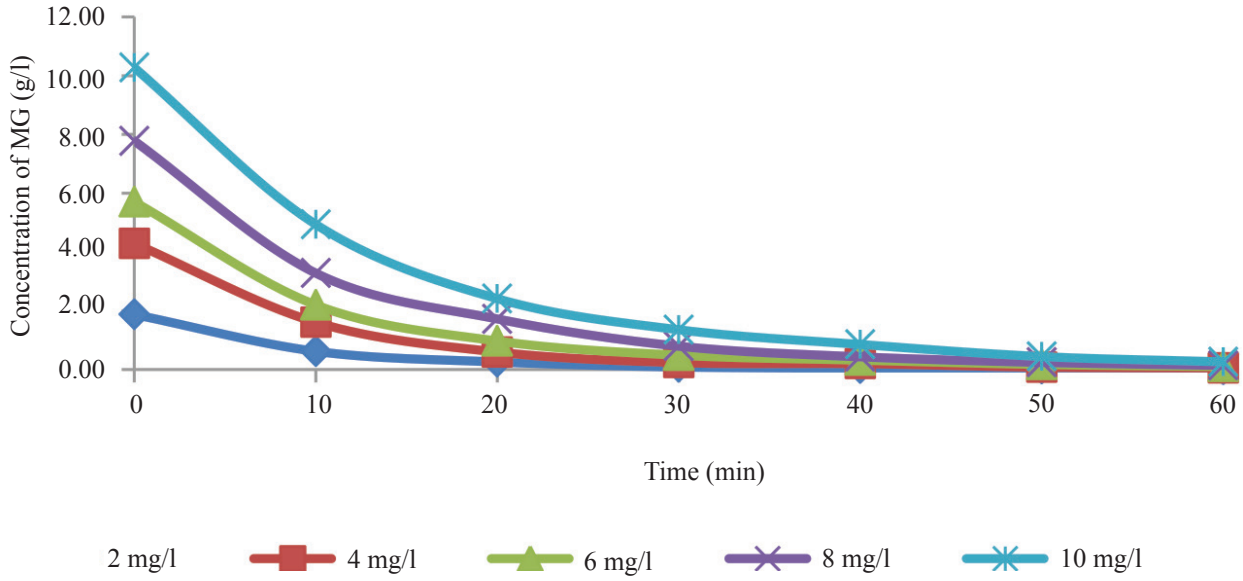


**Figure 4.** Initial Concentration of MG dye.

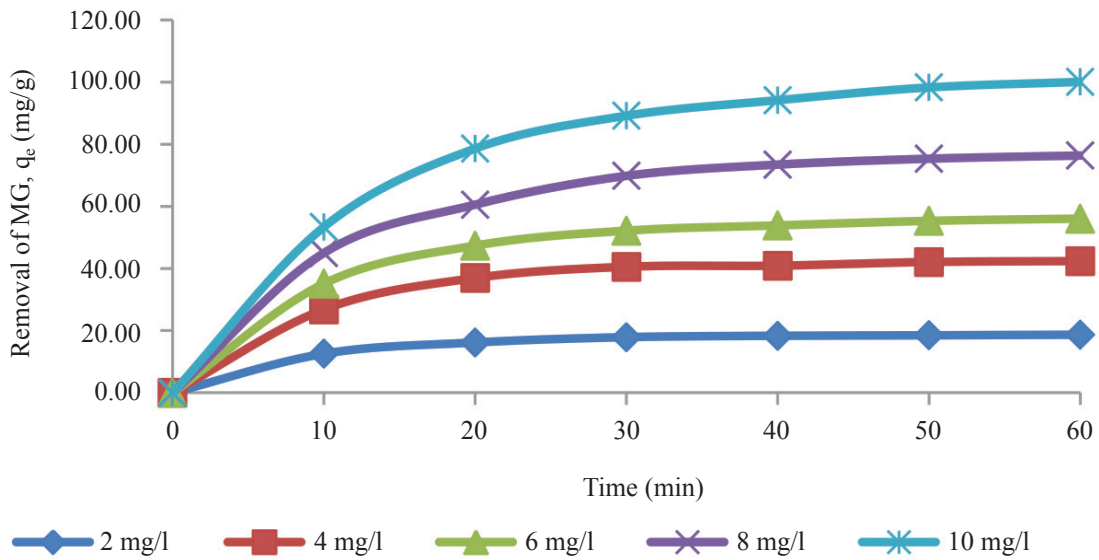


**Figure 5.** Adsorption of MG dye at various initial concentration.

driving force to overcome the mass transfer resistance for MG transfer between the solution and the surface of adsorbent.

**Adsorption Isotherm**

In this study, two well-known models of isotherms were compared in order to describe how the adsorbate molecules were distributed between the liquid and solid phases when the equilibrium was reached.

Langmuir isotherm is derived on the assumption of monolayer adsorption on a homogenous surface. It is expressed as in Equation 5 for linear equations [21].

$$\frac{C_e}{q_e} = \frac{1}{q_{\max} b} + \frac{C_e}{q_{\max}} \quad (5)$$

Where, $q_{\max}$ (mg/g) and $b$ (l/mg) are the Langmuir constants related to maximum monolayer capacity and energy of adsorption, respectively.

The fundamental characteristics of the Langmuir isotherm could be described using separation factor or equilibrium constant $R_L$. Its value indicated whether the isotherm were unfavourable ($R_L$>1), linear ($R_L$ = 1), favourable (0<$R_L$<1) or irreversible ($R_L$ = 0) [21]. $R_L$ value expressed as;

$$R_L = \frac{1}{(1+kC_0)} \quad (6)$$

Freundlich isotherm is suitable for non-ideal adsorption on homogeneous surface. The heterogeneity is caused by the presence of different functional groups on the surface, and several adsorbent–adsorbate interactions [21] and expressed as Equation 7 for linear equations:

$$\log q_e = n \log C_e + \log K_F \quad (7)$$

where $K_F$ (mg/g) (l/mg) is the Freundlich adsorption constant and 1/n is a measure of the adsorption intensity.

Figures 6 and 7 are the linear plot of Langmuir and Freundlich isotherm respectively. The data are fitted to both Langmuir and Freundlich isotherm. Based on Table 3, the regression coefficient, $R^2$, AC6 fitted Freundlich isotherm ($R^2$ = 0.9906) better than Langmuir isotherm ($R^2$ = 0.9062). This isotherm indicated that the adsorption of MG dye onto AC6 was favaurable for multilayer isotherm.

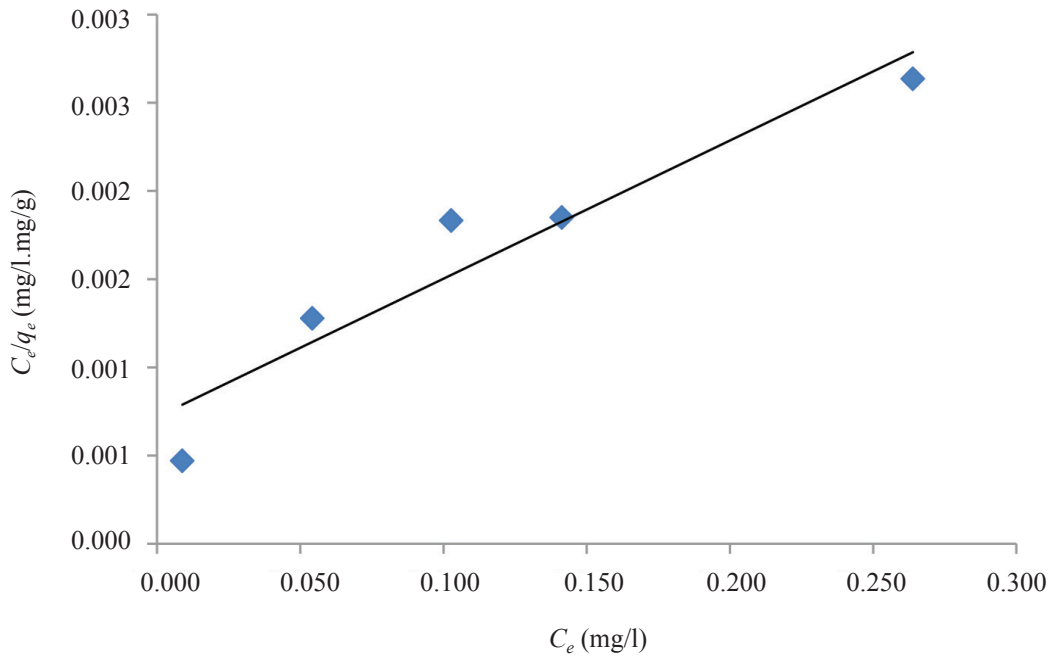


**Figure 6.** Langmuir isotherm for AC6.

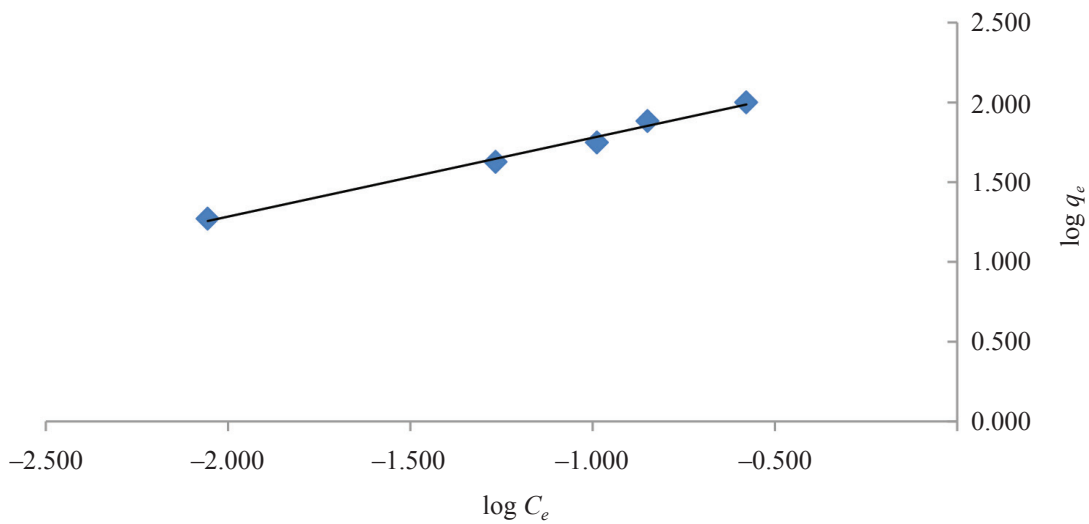


**Figure 7.** Freundlich isotherm for AC6.

**Table 3.** Adsorption isotherm of MG dye onto AC6.

| Langmuir isotherm | | | | Freundlich isotherm | | |
|---|---|---|---|---|---|---|
| $q_{max}$ (mg/g) | $b$(l/mg) | $R^2$ | $R_L$ | $K_f$ (mg/g)(l/mg) | n | $R^2$ |
| 128.21 | 11.14 | 0.9076 | 0.009 | 9.71 | 2.02 | 0.9906 |

**Adsorption Kinetics**

Adsorption kinetics describes the mechanisms of adsorption processes, which, in turn, control the equilibrium time and mass transfer of the adsorbates [24]. In order to study this kinetics, pseudo first order kinetics and pseudo second order kinetics were applied and linear forms of these equations were expressed as in Equation 8 and Equation 9, respectively.

$$\log (q_e - q_t) = \log q_e - k_1 t \quad (8)$$

$$\frac{t}{q_t} = \frac{t}{q_e} + \frac{1}{k_2 q_e^2} \quad (9)$$

Where $k_1$ is the rate constant of pseudo first-order model ($min^{-1}$), and $k_2$ is the rate constant of pseudo second-order model (g/mg min).

The suitability of the kinetic model to describe the adsorption process was further validated by the normal standard deviation, $\Delta q$ (%) defined as [31]:

$$\Delta q\ (\%) = \sqrt{\frac{\frac{(q_{e,\exp} - q_{e,\text{cal}})}{q_{e,\exp}}}{N-1}} \times 100 \quad (10)$$

Where, N is the number of data points, $q_{e,\exp}$ and $q_{e,\text{cal}}$ are the amount of MG adsorbed by both experimental and calculated, respectively.

The kinetics study of MG dye by AC6 were analysed using kinetics pseudo first and pseudo second order for linear model as illustrated in Figures 8 and 9 and the data was summarized in Table 4. Based on the data (Table 4), the kinetics study of AC6 fitted well with pseudo second order compared to pseudo first order kinetics. This could be clarified by the regression coefficient, $R^2$ value of pseudo second order is higher (>0.99) compared to pseudo first order kinetics (<0.99), while the calculated values of *qe*, cal (mg/g) from pseudo second order are much closer to the experimental value, *qe*, exp (mg/g) compared to pseudo first order. The consistency of the data was also supported by the value of $\Delta q$ (%) which showed that the pseudo second order has a smaller $\Delta q$ (%)(4.1% to 8.32%) than pseudo first order (6.3% to 20.34%). The rate of coefficient of pseudo second order, $k_2$, was found to decrease as initial concentration increased. This was related to the decrease of electrostatic interaction on the site, thus lowering the dyes affinity towards the adsorbent [32].

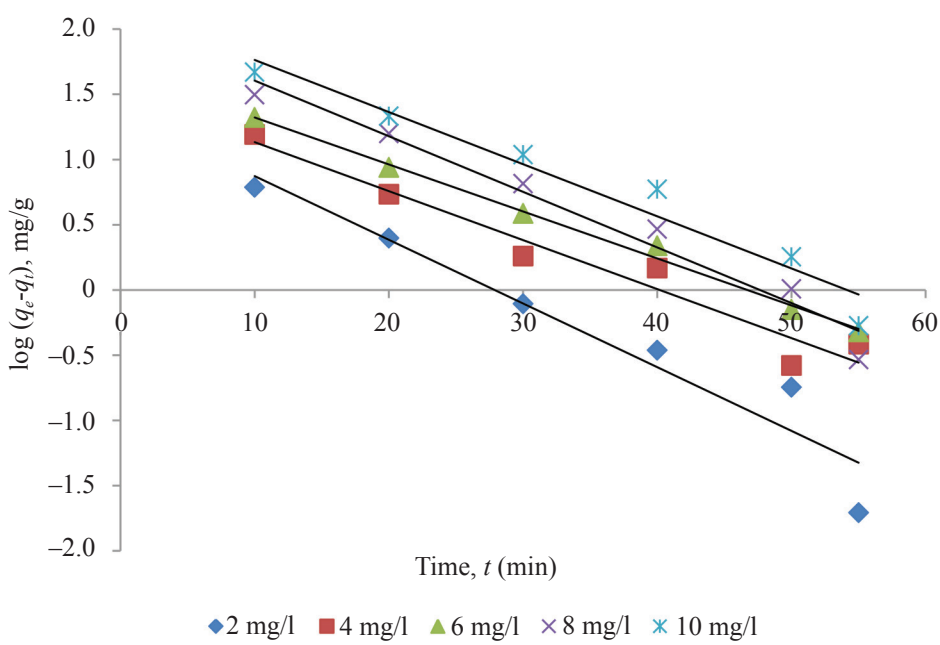


**Figure 8.** Kinetics pseudo first order.

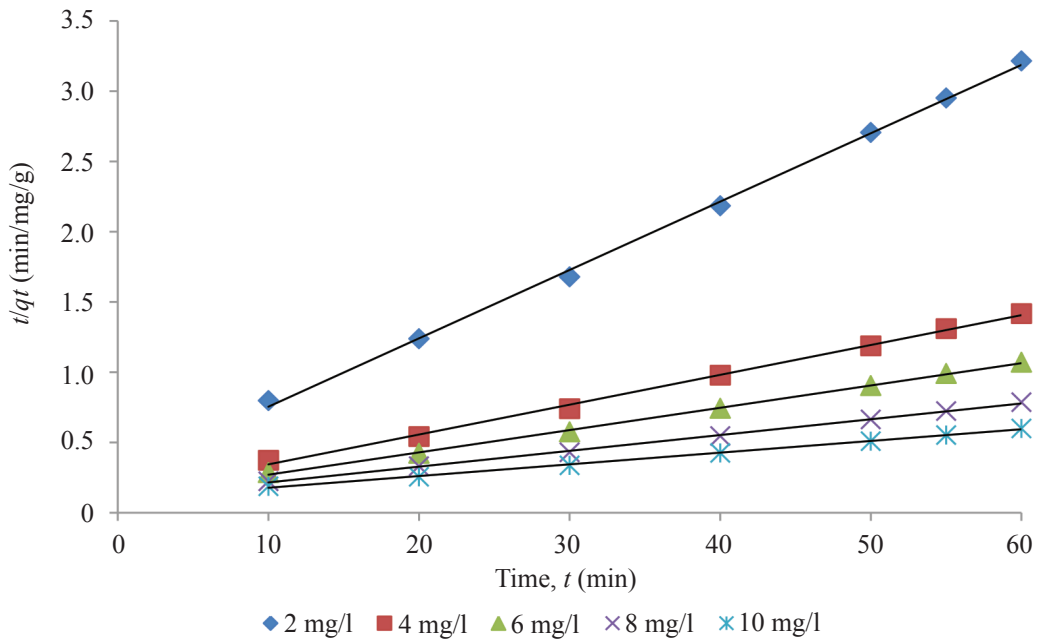


**Figure 9.** Kinetics pseudo second order.

**Table 4.** Adsorption kinetic study of MG dye onto AC6.

| Initial conc. (mg/l) | $q_{e,\exp}$ (mg/g) | Kinetic pseudo 1st order | | | | Kinetic pseudo 2nd order | | | |
|---|---|---|---|---|---|---|---|---|---|
| | | $q_{e,cal}$ (mg/g) | $k_1$ ($min^{-1}$) | $R^2$ | $\Delta q$% | $q_{e,cal}$ (mg/g) | $k_2$ $g(mgh)^{-1}$ | $R^2$ | $\Delta q$% |
| 2 | 18.67 | 23.01 | 0.113 | 0.9277 | 10.41 | 20.54 | 0.009 | 0.9988 | 4.1 |
| 4 | 42.37 | 32.31 | 0.087 | 0.9243 | 10.62 | 46.95 | 0.004 | 0.9977 | 4.43 |
| 6 | 56.05 | 48.17 | 0.083 | 0.9941 | 6.30 | 62.9 | 0.003 | 0.9990 | 4.99 |
| 8 | 76.37 | 90.47 | 0.091 | 0.9852 | 8.26 | 88.5 | 0.002 | 0.9989 | 6.49 |
| 10 | 100.09 | 145.62 | 0.093 | 0.9512 | 20.34 | 120.49 | 0.001 | 0.9984 | 8.32 |

## CONCLUSION

Activated carbon was prepared from waste tyre using NaOH as activating agent via $CO_2$ activation. The properties of activated carbon prepared were studied and the influence of impregnation ratio, activation temperature and time were investigated. The percentage of carbon produced decreased as impregnation ratio, temperature and time increased. AC1 produced the highest carbon yield, 76.09% compared to other samples, while AC6 was reported to have the highest surface area (313.75 $m^2/g$). Average moisture and ash content were in the range of 1.09% – 3.33% and 9.01% – 13.09%, respectively. AC6 prepared at impregnation ratio of 3:1 (NaOH:Char), activated at 900°C for 60 min was found to have the highest adsorption capacity, able to adsorb 97.43% of MG dye (100.09 mg/g) and was selected for further adsorption studies. Adsorption isotherm for AC6 fitted Freundlich isotherm which indicated a multilayer adsorption. The Langmuir maximum monolayer adsorption capacity was about 128.21 mg/g. Kinetic studies applied showed a best fit for pseudo second order kinetic with $R^2 > 0.99$ for all concentration and lowest number of $\Delta q$ (%) (4.1% to 8.32%).

## ACKNOWLEDGEMENT

This research was fully supported by the Centre of Research and Innovation, Universiti Malaysia Sabah (Grant No. SBK0058-SG-2013), and this support is gratefully acknowledged.

## REFERENCES

1. Dahri, M.K., Kooh, M.R.R. and Lim, L.B.L. (2014) Water remediation using low cost adsorbent walnut shell for removal of malachite green: Equilibrium, kinetics, thermodynamic and regeneration studies, *J. Environ. Chem. Eng.*, **2**, 1434–1444.
2. Tian, Y., Liu, P., Wang, X. and Lin, H. (2011) Adsorption of malachite green from aqueous solutions onto ordered mesoporous carbons, *Chem. Eng. J.*, **171**, 1263–1269.
3. Hamad, B.K., Noor, A.M., Afida, A.R. and Mohd Asri, M.N. (2010) High removal of 4-chloroguaiacol by high surface area of oil palm shell-activated carbon activated with NaOH from aqueous solution, *Desalination*, **257**, 1–7.
4. Williams, P.T. (2013) Pyrolysis of waste tyres: A review, *Waste Manag.*, **33**, 1714–1728.
5. Mui, E.L.K., Ko, D.C.K. and McKay, G. (2004) Production of active carbons from waste tyres—a review, *Carbon*, **42**, 2789–2805.
6. Hofman, M. and Pietrzak, R. (2011) Adsorbents obtained from waste tires for $NO_2$ removal under dry conditions at room temperature. *Chem. Eng. J.*, **170**, 202–208.
7. Martínez, J.D., Puy, N., Murillo, R., García, T., Navarro, M.V. and Mastral, A.M. (2013) Waste tyre pyrolysis — A review, *Renew. Sustain. Energy Rev.*, **23**, 179–213.
8. Joseph, C.G., Hoon, G.G., Sharain-Liew, Y.L., Krishnaiah, D. and Massuanna, M. (2013) Preparation and characterization of activated carbon derived from waste rubber tire via chemical activation with $ZnCl_2$: Surface area and morphological studies, in *Developments in Sustainable Chemical and Bioprocess Technology*, eds. R. Pogaku, A. Bono and C. Chu, Springer US.
9. Gupta, V.K., Nayak, A., Agarwal, S. and Tyagi, I. (2014) Potential of activated carbon from waste rubber tire for the adsorption of phenolics: Effect of pre-treatment conditions, *J. Colloid Interface Sci.*, **417**, 420–430.
10. Hamadi, N.K., Chen, X.D., Farid, M.M. and Lu, M.G.Q. (2001) Adsorption kinetics for the removal of chromium(VI) from aqueous solution by adsorbents derived from used tyres and sawdust, *Chem. Eng. J.*, **84**, 95–105.
11. Nakagawa, K., Namba, A., Mukai, S.R., Tamon, H., Ariyadejwanich, P. and Tanthapanichakoon, W. (2004) Adsorption of phenol and reactive dye from aqueous solution on activated carbons derived from solid wastes, *Water Res.*, **38**, 1791–1798.
12. Lian, F., Xing, B. and Zhu, L. (2011) Comparative study on composition, structure, and adsorption behavior of activated carbons derived from different synthetic waste polymers, *J. Colloid Interface Sci.*, **360**, 725–730.
13. Teng, H., Lin, Y.-C. and Hsu, L.-Y. (2000) Production of Activated Carbons from Pyrolysis of Waste Tires Impregnated with Potassium Hydroxide, *J. Air Waste Manag. Assoc.*, **50**, 1940–1946.
14. Gupta, V.K., Nayak, A. and Agarwal, S. (2012) Performance evaluation and application of oxygen enriched waste rubber tire adsorbent for the removal of hazardous aniline derivatives from waste water, *Chem. Eng. J.*, **203**, 447–457.
15. Pietrzak, R., Nowicki, P., Kaźmierczak, J., Kuszyńska, I., Goscianska, J. and Przepiórski, J. (2014) Comparison of the effects of different chemical activation methods on properties of carbonaceous adsorbents obtained from cherry stones, *Chem. Eng. Res. Des.*, **92**, 1187–1191.
16. Muniandy, L., Adam, F., Mohamed, A.R. and Ng, E.-P. (2014) The synthesis and characterization of high purity mixed microporous/mesoporous activated carbon from rice husk using chemical activation with NaOH and KOH, *Microporous Mesoporous Mater*, **197**, 316–323.
17. Hsu, S.-H., Huang, C.-S., Chung, T.-W. and Gao, S. (2014) Adsorption of chlorinated volatile organic compounds using activated carbon made from Jatropha curcas seeds, *J. Taiwan Inst. Chem. Eng.*, **45**, 2526–2530.
18. Wu, M., Guo, Q. and Fu, G. (2013) Preparation and characteristics of medicinal activated carbon powders by $CO_2$ activation of peanut shells, *Powder Technol.*, **247**, 188–196.
19. Cazetta, A.L., Vargas, A.M.M., Nogami, E.M., Kunita, M.H., Guilherme, M.R., Martins, A.C., Silva, T.L., Moraes, J.C.G. and Almeida, V.C.

(2011) NaOH-activated carbon of high surface area produced from coconut shell: Kinetics and equilibrium studies from the methylene blue adsorption, *Chem. Eng. J.*, **174**, 117–125.

20. SIRIM (1984) *Specification of Powder AC MS873*, Standardization and Industrial Research Institute Malaysia, Kuala Lumpur.
21. Hameed, B.H. and El-Khaiary, M.I. (2008) Equilibrium, kinetics and mechanism of malachite green adsorption on activated carbon prepared from bamboo by $K_2CO_3$ activation and subsequent gasification with $CO_2$, *J. Hazard. Mater.*, **157**, 344–351.
22. Anisuzzaman, S.M., Joseph, C.G., Taufiq-Yap, Y.H., Krishnaiah, D. and Tay, V.V. (2013) Modification of commercial activated carbon for the removal of 2,4-dichlorophenol from simulated wastewater, *J. King Saud Univ. - Sci.,* **25** (3), 251–255
23. Chan, O.S., Cheung, W.H. and McKay, G. (2011) Preparation and characterisation of demineralised tyre derived activated carbon, *Carbon*, **49**, 4674–4687.
24. Foo, K.Y. and Hameed, B.H. (2012) Textural porosity, surface chemistry and adsorptive properties of durian shell derived activated carbon prepared by microwave assisted NaOH activation, *Chem. Eng. J.*, **187**, 53–62.
25. Fernández, A.M., Barriocanal, C. and Alvarez, R. (2012) Pyrolysis of a waste from the grinding of scrap tyres, *J. Hazard. Mater.*, 203–204, 236–243.
26. Foo, K.Y. and Hameed, B.H. (2011) Microwave assisted preparation of activated carbon from pomelo skin for the removal of anionic and cationic dyes, *Chem. Eng. J.*, **173**, 385–390.
27. Saleh, T.A., Gupta, V.K. and Al-Saadi, A.A. (2013) Adsorption of lead ions from aqueous solution using porous carbon derived from rubber tires: Experimental and computational study, *J. Colloid Interface Sci.*, **396**, 264–269.
28. Tongpoothorn, W., Sriuttha, M., Homchan, P., Chanthai, S. and Ruangviriyachai, C. (2011) Preparation of activated carbon derived from Jatropha curcas fruit shell by simple thermo-chemical activation and characterization of their physico-chemical properties, *Chem. Eng. Res. Des.*, **89**, 335–340.
29. Undri, A., Meini, S., Rosi, L., Frediani, M. and Frediani, P. (2013) Microwave pyrolysis of polymeric materials: Waste tires treatment and characterization of the value-added products, *J. Anal. Appl. Pyrolysis*, **103**, 149–158.
30. Ghaedi, M., Shojaeipour, E., Ghaedi, A.M. and Sahraei, R. (2015) Isotherm and kinetics study of malachite green adsorption onto copper nanowires loaded on activated carbon: Artificial neural network modeling and genetic algorithm optimization, *Spectrochim. Acta. A. Mol. Biomol. Spectrosc.*, **142,** 135–149.
31. Foo, K.Y. and Hameed, B.H. (2012) Potential of jackfruit peel as precursor for activated carbon prepared by microwave induced NaOH activation, *Bioresour. Technol.*, **112**, 143–150.
32. Ahmad, M.A., Ahmad, N. and Bello, O.S. (2014) Adsorptive removal of malachite green dye using durian seed-based activated carbon, *Water, Air and Soil Pollution*, **225**, 2057–2074.